

# Dinuclear Gold(I) Dithiophosphonate Complexes: Synthesis, Luminescent Properties, and X-ray Crystal Structures of $[\text{Au}_2\text{S}_2\text{PR}(\text{OR}')_2]$ ( $\text{R} = \text{Ph}$ , $\text{R}' = \text{C}_5\text{H}_9$ ; $\text{R} = 4\text{-C}_6\text{H}_4\text{OMe}$ , $\text{R}' = (1S,5R,2S)\text{-(-)-Menthyl}$ ; $\text{R} = \text{Fc}$ , $\text{R}' = (\text{CH}_2)_2\text{O}(\text{CH}_2)_2\text{OMe}$ )

Werner E. van Zyl,<sup>†</sup> José M. López-de-Luzuriaga,<sup>‡</sup> Ahmed A. Mohamed,<sup>†</sup> Richard J. Staples,<sup>§</sup> and John P. Fackler, Jr.\*<sup>†</sup>

Department of Chemistry and Laboratory for Molecular Structure and Bonding, Texas A&M University, P.O. Box 30012, College Station, Texas 77842-3012, Departamento de Química, Grupo de Síntesis Química de La Rioja, Universidad de La Rioja, Madre de Dios 51, E-26004 Logroño, Spain, and Department of Chemistry and Chemical Biology, Harvard University, Cambridge, Massachusetts 02138

Received March 7, 2002

2,4-Diaryl- and 2,4-diferrocenyl-1,3-dithiadiphosphetane disulfide dimers  $(\text{RP}(\text{S})\text{S})_2$  ( $\text{R} = \text{Ph}$  (**1a**),  $4\text{-C}_6\text{H}_4\text{OMe}$  (**1b**),  $\text{Fc}$  (**1c**)) react with a variety of alcohols, silanols, and trialkylsilyl alcohols to form new dithiophosphonic acids in a facile manner. Their corresponding salts react with chlorogold(I) complexes in THF to produce dinuclear gold(I) dithiophosphonate complexes of the type  $[\text{Au}_2\text{S}_2\text{PR}(\text{OR}')_2]$  in satisfactory yield. The asymmetrical nature of the ligands allows for the gold complexes to form two isomers (cis and trans) as verified by solution  $^1\text{H}$  and  $^{31}\text{P}\{\text{H}\}$  NMR studies. The X-ray crystal structures of  $[\text{Au}_2\text{S}_2\text{PR}(\text{OR}')_2]$  ( $\text{R} = \text{Ph}$ ,  $\text{R}' = \text{C}_5\text{H}_9$  (**2**);  $\text{R} = 4\text{-C}_6\text{H}_4\text{OMe}$ ,  $\text{R}' = (1S,5R,2S)\text{-(-)-menthyl}$  (**3**);  $\text{R} = \text{Fc}$ ,  $\text{R}' = (\text{CH}_2)_2\text{O}(\text{CH}_2)_2\text{OMe}$  (**4**)) have been determined. In all cases only the trans isomer is obtained, consistent with solid state  $^{31}\text{P}$  NMR data obtained for the bulk powder of **3**. Crystallographic data for **2** (213 K): orthorhombic,  $Ibam$ ,  $a = 12.434(5)$  Å,  $b = 19.029(9)$  Å,  $c = 11.760(4)$  Å,  $V = 2782(2)$  Å<sup>3</sup>,  $Z = 4$ . Data for **3** (293 K): monoclinic,  $P2_1$ ,  $a = 7.288(2)$  Å,  $b = 12.676(3)$  Å,  $c = 21.826(4)$  Å,  $\beta = 92.04(3)^\circ$ ,  $V = 2015.0(7)$  Å<sup>3</sup>,  $Z = 2$ . Data for **4** (213 K): monoclinic,  $P2_1/n$ ,  $a = 11.8564(7)$  Å,  $b = 22.483(1)$  Å,  $c = 27.840(2)$  Å,  $\beta = 91.121(1)^\circ$ ,  $V = 7419.8(8)$  Å<sup>3</sup>,  $Z = 8$ . Moreover, **1a–c** react with  $[\text{Au}_2(\text{dppm})\text{Cl}_2]$  to form new heterobridged trithiophosphonate complexes of the type  $[\text{Au}_2(\text{dppm})(\text{S}_2\text{P}(\text{S})\text{R})]$  ( $\text{R} = \text{Fc}$  (**12**)). The luminescence properties of several structurally characterized complexes have been investigated. Each of the title compounds luminesces at 77 K. The results indicate that the nature of  $\text{Au}\cdots\text{Au}$  interactions in the solid state has a profound influence on the optical properties of these complexes.

## Introduction

In recent years, due to the potential application in electrochemistry,<sup>1</sup> microelectronics,<sup>2</sup> catalysis,<sup>3</sup> ion exchange,<sup>4</sup> sensors,<sup>5</sup> photophysics,<sup>6</sup> and materials,<sup>7</sup> metal phosphonate chemistry has flourished. In contrast, research

utilizing the related dithiophosphonate ligand,  $[\text{S}_2\text{PR}(\text{OR}')^-]$ , in metal complex formation has not been abundant. This is exemplified by the fact that few compounds that contain this ligand have been structurally characterized.<sup>8</sup> This is surprising since phosphorus-1,1-dithiolates as a general class of compounds have been important as antiwear and antioxidant additives in the oil and petroleum industry,<sup>9</sup> as agricultural insecticide derivatives,<sup>10</sup> and as metal ore extraction reagents.<sup>11</sup> As part of our ongoing studies of gold–sulfur compounds, we report here the chemistry derived from the reaction between these monoanionic, potentially bidentate sulfur ligands and gold(I), yielding dinuclear gold(I) dithio-

\* To whom correspondence should be addressed. E-mail: fackler@mail.chem.tamu.edu.

<sup>†</sup> Texas A&M University.

<sup>‡</sup> Universidad de La Rioja.

<sup>§</sup> Harvard University.

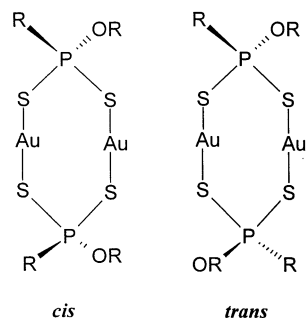
(1) Murray, R. W. *Acc. Chem. Res.* **1980**, *13*, 135.

(2) Roberts, G. G. *Adv. Phys.* **1985**, *34*, 475.

(3) Cheng, S.; Peng, G.-Z.; Clearfield, A. *Ind. Eng. Chem. Prod. Res. Dev.* **1984**, *23*, 2.

phosphonate complexes. A general synthetic route for dithiophosphonate salts has been described.<sup>12</sup>

We found that dithiophosphonates form an interesting modification of the known dithiophosphate chemistry. Although the ligands are not commercially available, a variety of new ligands is obtained in a facile manner from a common precursor. The asymmetrical nature of the ligand allows for two isomers (cis and trans) to be formed, a feature not possible for the symmetrical dithiophosphinates,  $[S_2PR_2]^-$ ,<sup>13</sup> or dithiophosphates,  $[S_2P(OR)_2]^-$ . The ligand also facilitates



the formation of an Au–S bond that is functionally well suited for photoluminescence studies. Indeed, these complexes possess a rich but complex photophysics. The results described here indicate that dinuclear gold(I) complexes with S–P–S bridging ligands have luminescent properties that are influenced strongly by the presence or absence of intermolecular Au···Au interactions. This observation appears to provide a means to determine whether *intermolecular* Au···Au interactions are present in the bulk sample independent of structural studies. Preliminary results related to this study have been reported previously.<sup>14</sup>

- (4) (a) Clearfield, A. In *New Developments in Ion Exchange Materials*; Abe, M., Kataoka, T., Suzuki, T., Eds.; Kodansha, Ltd.: Tokyo, 1991. (b) Wang, J. D.; Clearfield, A.; Peng, G.-Z. *Mater. Chem. Phys.* **1993**, *35*, 208.
- (5) Alberti, G.; Casciola, M.; Palombi, R. *Solid State Ionics* **1993**, *61*, 241.
- (6) (a) Vermeulen, L. A.; Thompson, M. E. *Nature* **1992**, *358*, 656. (b) Vermeulen, L. A.; Snover, J. L.; Sapochak, L. S.; Thompson, M. E. *J. Am. Chem. Soc.* **1993**, *115*, 11767.
- (7) Cao, G.; Hong, H.; Mallouk, T. E. *Acc. Chem. Res.* **1992**, *25*, 420.
- (8) (a) Fackler, J. P., Jr.; Thompson, L. D. *Inorg. Chim. Acta* **1981**, *45*. (b) Murray, H. H.; Garzón, G.; Raptis, R. G.; Mazany, A. M.; Porter, L. C.; Fackler, J. P., Jr. *Inorg. Chem.* **1988**, *27*, 836. (c) Bone, S. P.; Constantinescu, R.; Haiduc, I. *J. Chem. Res.* **1979**, S69. (d) Haiduc, I.; Sowerby, D. B.; Lu, S. F. *Polyhedron* **1995**, *14*, 3389–3472. (e) Fackler, J. P., Jr.; van Zyl, W. E.; Prihoda, B. A. In *Gold: Progress in Chemistry, Biochemistry and Technology*; Schmidbaur, H., Ed.; John Wiley & Sons: West Sussex, England, 1999; pp 795–840.
- (9) (a) Klamann, D., Ed. *Lubricants and Related Products*; Verlag Chemie: Weinheim, Germany, 1984. (b) Colclough T. *Ind. Eng. Chem.* **1987**, *26*, 1888. (c) Dumdum, J. M.; Mendelson, L. T.; Pilling, R. L. U.S. Pat. 4,908,142; *Chem. Abstr.* **1990**, *112*, 201925k.
- (10) Patnaik, P. *A Comprehensive Guide to the Hazardous Properties of Chemical Substances*; Van Nostrand Reinhold: New York, 1992; Chapter 40 and references therein.
- (11) Miyake, Y.; Harada, M. *Rev. Inorg. Chem.* **1989**, *10*, 145.
- (12) van Zyl, W. E.; Fackler, J. P., Jr. *Phosphorus, Sulfur Silicon* **2000**, *167*, 117–132.
- (13) van Zyl, W. E.; Lopez-de-Luzuriaga, J. M.; Fackler, J. P., Jr.; Staples, R. J. *Can J. Chem.* **2001**, *79*, 896–903.
- (14) (a) van Zyl, W. E.; Staples, R. J.; Fackler, J. P., Jr. *Inorg. Chem. Commun.* **1998**, *1*, 51. (b) van Zyl, W. E.; Lopez-de-Luzuriaga, J. M.; Fackler, J. P., Jr. *J. Mol. Struct.* **2000**, *516*, 99–106.

## Experimental Section

Caution! Tetrahydrothiophene has a foul smell and may cause conjunctivitis. Several organophosphorus compounds described herein are highly malodorous, and all are highly toxic. Manipulations of these materials should be performed in a well-ventilated fume hood. Hydrogen sulfide excess was destroyed by bubbling the gas through a dilute NaClO (bleach) solution.

**General Methods.** Unless otherwise noted, all reactions and manipulations were carried out under an inert atmosphere with a positive nitrogen gas flow using standard Schlenk techniques.<sup>15</sup> Diethyl ether, THF, benzene, and hexane were distilled under dinitrogen over a Na/K alloy with the formation of a benzophenone ketyl indicator. Dichloromethane was distilled over P<sub>4</sub>O<sub>10</sub>. Methanol and ethanol were distilled from Mg turnings.<sup>16</sup> The following chemicals were purchased from Aldrich Chemical Co.: tetrahydrothiophene; tetraphosphorus decasulfide; ferrocene; bis(diphenylphosphino)methane; cyclopentanol; cyclohexanol; allyl alcohol; (1*R*,2*S*,5*R*)-(–)-menthol; 2-(2-methoxyethoxy)ethanol; 1-adamantanol; trimethylsilyl alcohol; triphenylsilanol; 2,4,6-trimethylphenol. Phenyl dichlorophosphine was obtained from Strem Chemicals. Hydrogen sulfide and ammonia gases were obtained from Matheson Gas Products Co. The following compounds were prepared by literature procedures: [PhP(S)S]<sub>2</sub>;<sup>17</sup> [4-C<sub>6</sub>H<sub>4</sub>OMeP(S)S]<sub>2</sub> (also commercially available);<sup>18</sup> [FcP(S)S]<sub>2</sub>.<sup>19</sup> All chemicals were used as received.

**Instrumentation.** Melting points were measured on a Unimelt capillary melting point apparatus and are uncorrected. Positive fast atom bombardment (+FAB/DIP) (DIP = direct insertion probe) mass spectrometry<sup>20</sup> was carried out on a VG Analytical (Manchester, U.K.) 70S high-resolution, double-focusing mass spectrometer. Samples for analyses were prepared by dissolving the solid compound in an appropriate solvent with a nitrobenzyl alcohol (NBA) matrix added and placed on the DIP tip. The probe was then inserted into the instrument through a vacuum interlock. The sample was bombarded with 8 keV xenon primary particles from an Ion Tech FAB gun operating at an emission current of 2 mA. Data were collected by a VG11-250J data system. <sup>1</sup>H NMR spectra were obtained on a Varian XL-200 spectrometer or a Varian UnityPlus-300 spectrometer. <sup>1</sup>H NMR data are expressed in parts per million (ppm) downfield shift referenced internally to the residual proton impurity in the deuterated solvent and are reported as chemical shift position ( $\delta_H$ ), multiplicity (s = singlet, d = doublet, t = triplet, q = quartet, and m = multiplet), relative integral intensity, and assignment. <sup>31</sup>P{<sup>1</sup>H} NMR spectra were obtained on a Varian XL 200 MHz broad-band spectrometer operating at 81 MHz or on a Varian UnityPlus-300 spectrometer operating at 121 MHz with chemical shifts reported relative to a 85% H<sub>3</sub>PO<sub>4</sub> in D<sub>2</sub>O external standard solution. The solid state <sup>31</sup>P NMR spectrum of **3** was obtained using a Bruker MSL-300 spectrometer operating at ambient temperature with a 7 mm magic angle spinning (MAS) probe. Data were acquired using a 30° pulse for excitation with a proton decoupled field of 62.5 kHz during acquisition. The sample

- (15) Shriver D. F.; Drezdson, M. A. *The Manipulation of Air-Sensitive Compounds*, 2nd ed.; John Wiley & Sons: New York, 1986.
- (16) Perrin, D. D.; Armarego, W. L. F. *Purification of Laboratory Chemicals*; Pergamon Press: New York, 1988.
- (17) Chupp, J. P.; Newallis, P. E. *J. Org. Chem.* **1962**, 3832.
- (18) Pederson, B. S.; Scheibye, S.; Nilsson, N. H.; Lawesson, S. O. *Bull. Soc. Chim. Belg.* **1978**, 223.
- (19) Foreman, M. R. St. J.; Slawin, A. M. Z.; Woollins, J. D. *J. Chem. Soc., Dalton Trans.* **1996**, 3653.
- (20) (a) Barber, M.; Bordoli, R. S.; Elliot, G. J.; Sedgwick, R. D.; Tyler, A. N. *Anal. Chem.* **1982**, *54*, 645A. (b) Aberth, W.; Straub, K. M.; Burlingame, A. L. *Anal. Chem.* **1982**, *54*, 2029.

was spinning at 4083 Hz about the magic angle. Using a recycle delay of 30 s, 16 scans were acquired for signal averaging.

**Excitation and Emission Spectra.** Excitation and emission spectra were obtained using a SLM/AMINCO model 8100 spectrofluorometer using a xenon lamp. The radiation was filtered through a 0.10 M KNO<sub>2</sub> solution to reduce the amount of scattered light. Low-temperature measurements were made in a cryogenic device of local design. Collodion was used to attach the powder samples to the holder. The collodion was scanned for baseline subtraction.

**X-ray Crystallography.** Crystals used in the diffraction measurements at room temperature were mounted on the tip of a quartz fiber with fast adhesive glue. Single-crystal diffraction analyses were carried out on **3** using an automated Nicolet R3 diffractometer utilizing the Wyckoff scanning technique with graphite-monochromated Mo K $\alpha$  ( $\lambda = 0.71073$  Å) radiation. The unit cell was determined using search, center, index, and least-squares refine routines. The Laue class and lattice dimensions were verified by axial oscillation photography. The intensity data were corrected for absorption, Lorentz, and polarization effects. An empirical absorption correction based on  $\psi$  scans of five strong reflections spanning a range of  $2\theta$  values. All data processing were performed by a Data General Eclipse S140 minicomputer using a SHELXTL crystallographic computational package (version 5.1) and Siemens SHELXTL PLUS (Micro Vax II).<sup>21</sup> The systematic absences were consistent with the space group assigned. The crystal structures were solved using direct methods to determine the gold atom positions, while other atoms were located on difference Fourier maps. Structure refinements were carried out using SHELX-93. The position of the hydrogen atoms were calculated by assuming idealized geometries, C–H = 0.93 Å. Crystal data for complexes **2** and **4** were collected on a Siemens (Bruker) SMART CCD (charge-coupled device) based diffractometer equipped with a LT-2 low-temperature apparatus operating at 213 K. A suitable crystal was chosen and mounted on a glass fiber using grease. Data were measured using omega scans of 0.3°/frame for 30 s, such that a hemisphere was collected. A total of 1271 frames were collected with a final resolution of 0.75 Å. The first 50 frames were collected at the end of the data collection to monitor for decay. Cell parameters were retrieved using SMART software<sup>22</sup> and refined using SAINT on all observed reflections. Data reduction was performed using SAINT software<sup>23</sup> which corrects for Lorentz polarization and decay. Absorption corrections were applied (semiempirical from  $\psi$  scans) using SADABS<sup>24</sup> supplied by G. Sheldrick. The structures were solved by direct methods using the SHELXS-90<sup>25</sup> and SHELXS-97 programs and refined by least-squares methods on  $F^2$ .<sup>26</sup> All non-hydrogen atoms were refined anisotropically. The crystal used for the diffraction study showed no decomposition during data collection. Crystallographic data and results are listed in Table 4. Atomic coordinates and thermal parameters for all structures are supplied as Supporting Information.

(21) Sheldrick, G. M. *SHELXTL-Plus User's Manual*; Nicolet XRD Corp.: Madison, WI, 1988.

(22) *SMART V 4.043 Software for the CCD Detector System*; Bruker Analytical X-ray Systems: Madison, WI, 1995.

(23) *SAINT V 4.035 Software for the CCD Detector System*; Bruker Analytical X-ray Systems: Madison, WI, 1995.

(24) Blessing, R. H. SADABS. Program for absorption corrections using Siemens CCD based on the method of Robert Blessing. *Acta Crystallogr.* **1995**, *A51*, 33.

(25) Sheldrick, G. M. *SHELXS-90, Program for the Solution of Crystal Structure*; University of Göttingen: Göttingen, Germany, 1990.

(26) Sheldrick, G. M. *SHELXL-97, Program for the Refinement of Crystal Structure*; University of Göttingen: Göttingen, Germany, 1997.

**Table 1.** Selected Bond Lengths (Å) and Angles (deg) for [Au<sub>2</sub>PPh(OC<sub>5</sub>H<sub>9</sub>)<sub>2</sub>], **2**

Au(1)–Au(1B)	2.9261(11)	S(1)–P(1)	2.002(2)
Au(1)–Au(1A)	2.9538(11)	P(1)–O(1)	1.553(7)
Au(1)–S(1E)	2.300(2)	P(1)–C(4)	1.811(10)
Au(1)–S(1)	2.300(2)	O(1)–C(1)	1.433(13)
S(1E)–Au(1)–S(1)	169.09(7)	P(1)–S(1)–Au(1)	104.38(9)
S(1E)–Au(1)–Au(1B)	84.55(4)	O(1)–P(1)–C(4)	101.0(4)
S(1)–Au(1)–Au(1B)	84.55(4)	O(1)–P(1)–S(1)	112.91(14)
S(1E)–Au(1)–Au(1A)	95.45(4)	C(4)–P(1)–S(1)	106.4(2)
S(1)–Au(1)–Au(1A)	95.45(4)	S(1)–P(1)–S(1B)	115.72(13)
Au(1A)–Au(1)–Au(1B)	180.0		

**Table 2.** Selected Bond Lengths (Å) and Angles (deg) for [Au<sub>2</sub>S<sub>2</sub>P(4-C<sub>6</sub>H<sub>4</sub>OMe)(O-menthyl)]<sub>2</sub>, **3**

Au(1)–S(1A)	2.297(6)	S(1)–P(1)	2.012(8)
Au(1)–S(2A)	2.303(6)	S(2)–P(2)	2.000(8)
Au(1)–Au(2)	3.0432(13)	P(2)–O(2)	1.595(14)
Au(2)–S(2)	2.288(6)	P(2)–C(21)	1.83(2)
Au(2)–S(1)	2.295(6)	O(1)–C(1)	1.51(2)
S(1A)–Au(1)–S(2A)	167.8(2)	S(2)–Au(2)–Au(1)	88.91(14)
S(1A)–Au(1)–Au(2)	94.72(14)	P(1)–S(1)–Au(2)	97.4(3)
S(2A)–Au(1)–Au(2)	97.44(14)	O(2)–P(2)–C(21)	109.2(8)
S(2)–Au(2)–S(1)	176.4(2)		

**Table 3.** Selected Bond Lengths (Å) and Angles (deg) for [Au<sub>2</sub>S<sub>2</sub>PFc(O(CH<sub>2</sub>)<sub>2</sub>O(CH<sub>2</sub>)<sub>2</sub>OMe)]<sub>2</sub>, **4**

Au(1)–S(1)	2.301(4)	S(1)–P(1)	2.021(6)
Au(1)–S(3)	2.318(4)	P(1)–O(1)	1.611(10)
Au(2)–Au(3)	3.0396(10)	P(1)–C(21)	1.770(15)
Au(1)–Au(2)	3.2355(9)	O(1)–C(1)	1.450(16)
Au(3)–Au(4)	3.0791(9)	Fe(2)–C(27)	1.985(16)
Au(2)–S(4)	2.307(4)	Fe(2)–C(30)	2.047(17)
Au(2)–S(2)	2.312(4)		
S(1)–Au(1)–S(3)	176.09(16)	S(3)–P(2)–S(4)	118.00(3)
S(1)–Au(1)–Au(2)	93.17(11)	S(7)–P(4)–S(8)	118.04(2)
Au(1)–Au(2)–Au(3)	171.19(3)	S(2)–Au(2)···Au(3)	83.57(11)
Au(2)–Au(3)–Au(4)	138.16(3)	Au(2)···Au(3)–S(7)	78.86(11)

**Materials.** The preparation of the ligand [NH<sub>4</sub>][S<sub>2</sub>PPh(OCH<sub>2</sub>CH=CH<sub>2</sub>)] is described below and is representative for preparing all the dithiophosphonic salt derivatives from **1a,b** precursors.<sup>12</sup>

It should be noted that analytical results were obtained<sup>12</sup> for the ammonium salt precursors to the gold products reported in this study.

[NH<sub>4</sub>][S<sub>2</sub>PPh(OCH<sub>2</sub>CH=CH<sub>2</sub>)]. A 25 mL Schlenk tube was charged with [PhP(S)S]<sub>2</sub>, **1a** (2.08 g, 6.01 mmol), and placed under vacuum for 30 min. The solid was heated to ~70 °C, and allyl alcohol (0.70 g, 12.02 mmol) was added and allowed to react. The temperature was maintained at 70–75 °C until dissolution of all the solids was observed and then stirred for an additional 20 min. The acids are typically volatile, viscous yellow colored oils. No attempt was made to isolate the acids. A small amount of benzene was added to the acid. The solution was placed in an ice bath for 10 min. Anhydrous ammonia gas was slowly bubbled through the solution with stirring. A colorless precipitate was formed immediately. In cases where the salt was sparingly soluble in benzene, precipitation was induced by evaporation of the solvent under reduced pressure. The material was filtered under aerobic conditions on a glass frit and washed with three 5 mL portions of cold hexane. The salts were dried in air yielding a free flowing, odorless, and colorless powder. In cases where the alcohol is a solid, it is dissolved in a minimum amount of benzene prior to addition. A slight excess of alcohol and/or a slightly elevated temperature ( $\leq 85$  °C) did not negatively reduce product purity or yield. Yield: 1.30 g (88%). Mp: 130 °C. The salts slowly hydrolyze in air and moisture but can be safely stored in a vacuum desiccator.

**Table 4.** Crystal Data and Structure Refinement for Complexes 2–4

	2	3	4
empirical formula	C <sub>22</sub> H <sub>28</sub> Au <sub>2</sub> O <sub>2</sub> P <sub>2</sub> S <sub>4</sub>	C <sub>34</sub> H <sub>52</sub> Au <sub>2</sub> O <sub>4</sub> P <sub>2</sub> S <sub>4</sub>	C <sub>30</sub> H <sub>40</sub> Au <sub>2</sub> O <sub>6</sub> P <sub>2</sub> S <sub>4</sub> Fe <sub>2</sub>
fw	908.56	1108.87	1192.43
temp (K)	213(2)	293(2)	213(2)
wavelength (Å)	0.710 73	0.710 73	0.710 73
cryst system	orthorhombic	monoclinic	monoclinic
space group	Ibam	P2 <sub>1</sub>	P2 <sub>1</sub> /n
unit cell dimens (Å, deg)	<i>a</i> = 12.434(5), $\alpha$ = 90 <i>b</i> = 19.029(9), $\beta$ = 90 <i>c</i> = 11.760(4), $\gamma$ = 90	<i>a</i> = 7.288(2), $\alpha$ = 90 <i>b</i> = 12.676(3), $\beta$ = 92.04(3) <i>c</i> = 21.826(4), $\gamma$ = 90	<i>a</i> = 11.8564(7), $\alpha$ = 90 <i>b</i> = 22.483(1), $\beta$ = 91.121(3) <i>c</i> = 27.840(2), $\gamma$ = 90
<i>V</i> (Å <sup>3</sup> ), <i>Z</i>	2782(2), 4	2015.0(7), 2	7419.8(8), 8
<i>D</i> (calcd) (g/cm <sup>3</sup> )	2.169	1.828	2.135
abs coeff (mm <sup>-1</sup> )	10.967	7.593	9.002
<i>F</i> (000)	1712	1080	4576
cryst size (mm)	0.15 × 0.10 × 0.05	0.20 × 0.20 × 0.15	0.05 × 0.10 × 0.30
$\theta$ range for data collcn (deg)	1.96–27.62	2.46–22.62	1.46–22.50
limiting indices	−15 ≤ <i>h</i> ≤ 15, −24 ≤ <i>k</i> ≤ 21, −12 ≤ <i>l</i> ≤ 14	0 ≤ <i>h</i> ≤ 7, 0 ≤ <i>k</i> ≤ 13, −23 ≤ <i>l</i> ≤ 23	−12 ≤ <i>h</i> ≤ 10, −24 ≤ <i>k</i> ≤ 24, −29 ≤ <i>l</i> ≤ 29
reflens colled	6374	2869	44 299
indpdt reflens	1606 [R(int) = 0.0419]	2634 [R(int) = 0.0389]	9701 [R(int) = 0.1592]
abs corr	semiempirical from $\psi$ scans	semiempirical from $\psi$ scans	semiempirical from $\psi$ scans
refinement method	full-matrix least squares on <i>F</i> <sup>2</sup>	full-matrix least squares on <i>F</i> <sup>2</sup>	full-matrix least squares on <i>F</i> <sup>2</sup>
data/restraints/params	1606/0/81	2634/97/406	9701/14/481
goodness-of-fit on <i>F</i> <sup>2</sup>	1.151	1.191	1.030
final R indices [ <i>I</i> > 2 $\sigma$ ( <i>I</i> )]	R1 = 0.0319, wR2 = 0.0898	R1 = 0.0410, wR2 = 0.0975	R1 = 0.0515, wR2 = 0.0738
R indices (all data)	R1 = 0.0390, wR2 = 0.0952	R1 = 0.0458, wR2 = 0.1015	R1 = 0.1300, wR2 = 0.0838
largest diff peak and hole (e <sup>-</sup> Å <sup>-3</sup> )	1.099 and −0.894	1.058 and −0.800	1.420 and −1.224

The gold(I) complexes **3–11** are formed in a fashion similar to the synthesis described for **2** given here.

**[AuS<sub>2</sub>PPh(OC<sub>5</sub>H<sub>9</sub>)<sub>2</sub>]<sub>2</sub>, 2.** A 50 mL Schlenk tube was charged with [NH<sub>4</sub>][S<sub>2</sub>PPh(OC<sub>5</sub>H<sub>9</sub>)<sub>2</sub>] (88 mg, 0.32 mmol) and placed under vacuum for 30 min. The salt was dissolved in 20 mL of THF, and upon dissolution Au(THT)Cl (THT = tetrahydrothiophene)<sup>27</sup> (100 mg, 0.31 mmol) was added in one portion at room temperature. An immediate white precipitate (NH<sub>4</sub>Cl) was observed. The mixture was stirred for 40 min followed by removal of the solvent in vacuo. The complex was extracted with CH<sub>2</sub>Cl<sub>2</sub> (25 mL) and filtered through anhydrous MgSO<sub>4</sub> to remove NH<sub>4</sub>Cl. The filtrate was evaporated under reduced pressure, which gave a pale yellow powder. The crude material was washed with three 10 mL portions of ether and dried under vacuum (10<sup>-2</sup> Torr) for 1 h. Yield: 70%. Mp: 186 °C (dec, green to brown). +FAB/DIP MS (NBA/CH<sub>2</sub>Cl<sub>2</sub>, *m/z*): 909 ([M + 1]<sup>+</sup>). <sup>1</sup>H NMR data for cis and trans isomers (chloroform-*d*, 300 MHz, 20 °C,  $\delta$ ): 8.12–8.02 (m, 4H, Ph), 7.54–7.39 (m, 6H, Ph), 1.95–1.45 (m, 18H, C<sub>5</sub>H<sub>9</sub>). <sup>31</sup>P{<sup>1</sup>H} NMR data (chloroform-*d*, 300 MHz, 20 °C,  $\delta$ ): 102.25 (s), 99.32 (s). Green crystals suitable for X-ray studies were obtained from the slow diffusion of hexane into a concentrated CH<sub>2</sub>Cl<sub>2</sub> solution. The complex is soluble in chlorinated solvents.

**[AuS<sub>2</sub>P(4-C<sub>6</sub>H<sub>4</sub>OCH<sub>3</sub>)(O-menthyl)<sub>2</sub>]<sub>2</sub>, 3.** Yield: 64%. Mp: 200 °C. +FAB/DIP MS (NBA/CHCl<sub>3</sub>, *m/z*): 1109 ([M + 1]<sup>+</sup>). <sup>1</sup>H NMR data for cis and trans isomers (chloroform-*d*, 300 MHz, 20 °C,  $\delta$ ): 8.18–7.90 (m, 2H, Ph), 7.00–6.85 (m, 2H, Ph), 3.87 (s-br, 3H, OCH<sub>3</sub>), 2.52–2.08 (m, 2H, CH), 1.72–1.58 (m, 2H, CH), 1.48–1.28 (m, 3H, CH), 1.20–0.98 (m, 3H, CH), 0.96–0.75 (m, 9H, CH<sub>3</sub>). <sup>31</sup>P{<sup>1</sup>H} NMR data (chloroform-*d*, 300 MHz, 20 °C,  $\delta$ ): 101.65 (s), 99.66 (s). <sup>31</sup>P{<sup>1</sup>H} NMR data (chloroform-*d*,  $\mu$ /D = 1.04 (g), 300 MHz, 20 °C,  $\delta$ ): 101.65 (s), 99.66 (s), with relative intensities of 0.57 and 1.00, respectively. Upon dissolution of the compound in acetonitrile (dipole moment,  $\mu$ /D (g) = 3.92), the <sup>31</sup>P{<sup>1</sup>H} NMR spectrum at 20 °C produces resonances at 103.97 and 102.51 with relative intensities of 0.82 and 1.00. In DMSO,  $\mu$ /D (g) = 3.96, and peaks at 103.65 and 102.18 are observed with relative intensities of 0.77 and 1.00, respectively. Colorless crystals suitable for X-ray studies were obtained from the slow evaporation

of an initially dilute CH<sub>2</sub>Cl<sub>2</sub> solution. Colorless crystals suitable for X-ray studies were obtained from the slow evaporation of an initially dilute CH<sub>2</sub>Cl<sub>2</sub> solution.

**[AuS<sub>2</sub>P(Fc)(O(CH<sub>2</sub>)<sub>2</sub>O(CH<sub>2</sub>)<sub>2</sub>OCH<sub>3</sub>)<sub>2</sub>]<sub>2</sub>, 4.** Yield: 58%. Mp: 106 °C. +FAB/DIP MS (NBA/CHCl<sub>3</sub>, *m/z*): 1192 ([M]<sup>+</sup>). <sup>1</sup>H NMR data for cis and trans isomers (chloroform-*d*, 300 MHz, 20 °C,  $\delta$ ): 4.69 (m, 2H, C<sub>5</sub>H<sub>4</sub>), 4.50 (m, 2H, C<sub>5</sub>H<sub>4</sub>), 4.38 (s, 5H, Cp), 3.95–3.52 (m, 8H, O(CH<sub>2</sub>)<sub>2</sub>O(CH<sub>2</sub>)<sub>2</sub>). <sup>31</sup>P{<sup>1</sup>H} NMR data (chloroform-*d*, 300 MHz, 20 °C,  $\delta$ ): 110.89 (s), 106.94 (s). Orange needles suitable for X-ray crystallographic study were obtained in a manner similar to that for **2**.

**[AuS<sub>2</sub>P(4-C<sub>6</sub>H<sub>4</sub>OCH<sub>3</sub>)(OSiPh<sub>3</sub>)<sub>2</sub>]<sub>2</sub>, 5.** Yield: 77%. Mp: 202 °C (dec). +FAB/DIP MS (NBA/CH<sub>2</sub>Cl<sub>2</sub>, *m/z*): 1349 ([M + 1]<sup>+</sup>), 1271 ([M – Ph]<sup>+</sup>). <sup>1</sup>H NMR data for the cis and trans isomers (chloroform-*d*, 300 MHz, 20 °C,  $\delta$ ): 7.94–7.84 (m, 4H, HCCO), 7.74–7.62 (m, 12H, SiPh<sub>3</sub>), 7.48–7.32 (m, 18H, SiPh<sub>3</sub>), 6.76–6.68 (m, 4H, HCCP), 3.81 (s, 6H, OCH<sub>3</sub>), 3.80 (s, 6H, OCH<sub>3</sub>). <sup>31</sup>P{<sup>1</sup>H} NMR data (chloroform-*d*, 300 MHz, 20 °C,  $\delta$ ): 93.01 (s), 90.28 (s). Colorless block crystals were obtained from a CH<sub>2</sub>Cl<sub>2</sub> solution layered with hexane within 24 h.

**[AuS<sub>2</sub>PPh(OEt)<sub>2</sub>]<sub>2</sub>, 6.** Yield: 185 mg, colorless (72%). Mp: 171 °C. +FAB/DIP MS (NBA/CHCl<sub>3</sub>, *m/z*): 829 ([M + 1]<sup>+</sup>), 631 ([M – Au]<sup>+</sup>). <sup>1</sup>H NMR data for cis and trans isomers (chloroform-*d*, 300 MHz, 20 °C,  $\delta$ ): 8.13–8.02 (m, 4H, Ph), 7.62–7.45 (m, 6H, Ph), 4.47 (q, 4H, OCH<sub>2</sub>), 4.42 (q, 4H, OCH<sub>2</sub>), 1.47 (t, 6H, CH<sub>3</sub>), 1.42 (t, 6H, CH<sub>3</sub>). <sup>31</sup>P{<sup>1</sup>H} NMR data (chloroform-*d*, 300 MHz, 20 °C,  $\delta$ ): 104.59 (s), 101.86 (s).

**[AuS<sub>2</sub>PPh(OCH<sub>2</sub>CH=CH<sub>2</sub>)<sub>2</sub>]<sub>2</sub>, 7.** Yield: 82%. Mp: 144 °C. +FAB/DIP MS (NBA/CHCl<sub>3</sub>, *m/z*): 853 ([M + 1]<sup>+</sup>), 655 ([M – Au]<sup>+</sup>), 427 ([M – AuL]<sup>+</sup>). <sup>1</sup>H NMR data for cis and trans isomers (chloroform-*d*, 300 MHz, 20 °C,  $\delta$ ): 8.11–8.01 (m, 4H, Ph), 7.61–7.44 (m, 6H, Ph), 6.10–5.90 (m-br, 2H, CH=CH<sub>2</sub>), 5.46 (d, 4H, OCH<sub>2</sub>), 5.30 (d, 4H, OCH<sub>2</sub>), 4.88 (s br, 4H, C=CH<sub>2</sub>). <sup>31</sup>P{<sup>1</sup>H} NMR data ( $\delta$ ): chloroform-*d*, 200 MHz, 19 °C, 106.18 (s), 103.37 (s); dichloromethane-*d*<sub>2</sub>, 200 MHz, 19 °C, 106.67 (s), 104.12 (s); deuterium oxide, 300 MHz, 22 °C, 106.72 (s), 104.21 (s). The pale yellow complex is soluble in chlorinated solvents.

**[AuS<sub>2</sub>PPh(OC<sub>6</sub>H<sub>11</sub>)<sub>2</sub>]<sub>2</sub>, 8.** Yield: 76%. Mp: 152 °C. +FAB/DIP MS (NBA/Na/CH<sub>2</sub>Cl<sub>2</sub>, *m/z*): 956 ([M + Na]<sup>+</sup>), 935 ([M + 1]<sup>+</sup>).

(27) Usón, R.; Laguna, A.; Laguna, M. *Inorg. Synth.* **1986**, *26*, 85.

$^1\text{H}$  NMR data for cis and trans isomers (chloroform-*d*, 300 MHz, 20 °C,  $\delta$ ): 8.22–8.00 (m, 4H, Ph), 7.60–7.40 (m, 6H, Ph), 1.80–1.20 (m, 22H,  $\text{OC}_6\text{H}_{11}$ ).  $^{31}\text{P}\{^1\text{H}\}$  NMR data (chloroform-*d*, 200 MHz, 20 °C,  $\delta$ ): 102.29 (s), 99.56 (s). The material is colorless and soluble in chlorinated solvents.

$[\text{Au}_2\text{PPh}(\text{O-adamantyl})_2]_2$ , **9**. Yield: 77%, colorless. Mp: 200 °C (dec, starts to foam from ca. 150 °C). +FAB/DIP MS (NBA/ $\text{CHCl}_3$ ,  $m/z$ ): 1041 ( $[\text{M} + 1]^+$ ).  $^1\text{H}$  NMR data for cis and trans isomers (chloroform-*d*, 200 MHz, 19.7 °C,  $\delta$ ): 8.30–8.08 (m, 4H, Ph), 7.58–7.38 (m, 6H, Ph), 2.28–2.03 (m, 9H, adamantyl), 1.62–1.44 (m, 6H, adamantyl).  $^{31}\text{P}\{^1\text{H}\}$  NMR data ( $\delta$ ): chloroform-*d*, 300 MHz, 22 °C, 96.03 (s), 95.62 (s); chloroform-*d*, 300 MHz, 40 °C, 96.09 (s), 95.68 (s).

$[\text{Au}_2\text{P}(4\text{-C}_6\text{H}_4\text{OCH}_3)(\text{OCH}_2\text{SiMe}_3)_2]_2$ , **10**. Yield: 80%, pale yellow. Mp: 158 °C. +FAB/DIP MS (NBA/EtOAc,  $m/z$ ): 1005 ( $[\text{M} + 1]^+$ ).  $^1\text{H}$  NMR data for cis and trans isomers (chloroform-*d*, 200 MHz, 19.7 °C,  $\delta$ ): 8.10–7.88 (m, 4H, Ph), 7.00–6.88 (m, 4H, Ph), 4.00 (d, 4H,  $\text{OCH}_2$ ), 3.92 (d, 4H,  $\text{OCH}_2$ ), 3.84 (s, 6H,  $\text{OCH}_3$ ), 3.83 (s, 6H,  $\text{OCH}_3$ ), 0.15 (s, 18H,  $\text{Si}(\text{CH}_3)_3$ ).  $^{31}\text{P}\{^1\text{H}\}$  NMR data (chloroform-*d*, 200 MHz, 19 °C,  $\delta$ ): 109.99 (s), 106.73 (s).

$[\text{Au}_2\text{PPh}(\text{OC}_6\text{H}_2(\text{CH}_3)_3)_2]_2$ , **11**. Yield: 62%, pale yellow. Mp: 214 °C.  $^1\text{H}$  NMR data for cis and trans isomers (chloroform-*d*, 300 MHz, 20 °C,  $\delta$ ): 8.26–8.14 (m, 2H, Ph), 7.60–7.40 (m, 3H, Ph), 6.81–6.79 (m, 2H, arom-mesityl), 2.34–2.20 (m, 9H,  $\text{CH}_3$ ).  $^{31}\text{P}\{^1\text{H}\}$  NMR data (chloroform-*d*, 300 MHz, 20 °C,  $\delta$ ): 105.76 (s), 105.12 (s). No FAB MS data collection was attempted. The complex is soluble in chlorinated solvents.

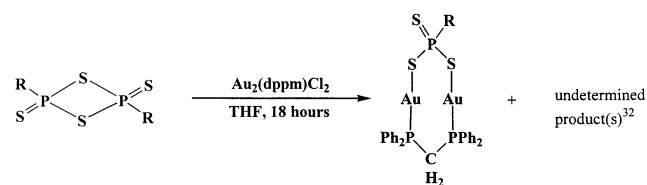
$[\text{Au}_2(\text{dppm})(\text{S}_2\text{P}(\text{S})\text{Fc})]_2$ , **12**. A 50 mL Schlenk tube was charged with  $[\text{FcP}(\text{S})\text{S}]_2$  (1.0 mmol), and 10 mL of THF was added.  $[\text{Au}_2(\text{dppm})\text{Cl}_2]$  (1.1 mmol) was added in one portion. The mixture was stirred for 18 h. The solution became clear after 1 h of stirring and depending on the concentration of the solution either remains that way (dilute solution) or yields a yellow precipitate (concentrated solution) after ~6 h of stirring. After 18 h, the THF was removed in vacuo. When the solution became concentrated, ether was added to induce complete precipitation of the product. The product was filtered on a frit, washed with cold ether, and air-dried. Yield: 71%. Mp: ~180 °C. +FAB/DP MS (NBA/Na/ $\text{CHCl}_3$ ,  $m/z$ ): 905 ( $[\text{M} - \text{FeC}_{10}\text{H}_9]^+$ ), 811 ( $[\text{M} - \text{S}_2\text{P}(\text{FeC}_{10}\text{H}_9)]^+$ ).  $^1\text{H}$  NMR data (dichloromethane-*d*<sub>2</sub>, 300 MHz, 20 °C,  $\delta$ ): 7.70–7.59 (m, 8H, Ph), 7.44–7.28 (m, 12H, Ph), 4.66 (q, 2H,  $\text{C}_5\text{H}_4$ ), 4.47 (q, 2H,  $\text{C}_5\text{H}_4$ ), 4.38 (s, 5H, Cp), 4.25 (t, 2H,  $\text{PCH}_2\text{P}$ ). A satisfactory  $^{31}\text{P}\{^1\text{H}\}$  NMR spectrum could not be obtained due to the poor solubility of the complex. The product is orange in single crystal form and yellow in powder form.

## Results and Discussion

**Synthesis.** A drawback in metal dithiophosphonate chemistry, and perhaps a reason for its paucity in the chemical literature, is that (unlike the phosphonates) the ligands are not readily available. It is known that 2,4-diaryl-1,3-dithiadiphosphetane disulfide dimers,  $(\text{RP}(\text{S})\text{S})_2$  ( $\text{R} = \text{Ph}$ , **1a**), react with two stoichiometric equiv of alcohol ( $\text{R}'\text{OH}$ ) at elevated temperatures (60–80 °C) to form dithiophosphonic acids,  $\text{HSP}(\text{S})\text{R}(\text{OR}')$ ,<sup>28</sup> through symmetric cleavage of the dimer. However, **1a** is formed from the reaction between  $\text{PhP}(\text{S})\text{Cl}_2$  and  $\text{H}_2\text{S}$  gas which is introduced sub-surface above 210 °C, with the ensuing reaction being very exothermic. Formation of **1a** through this route is thus cumbersome and hazardous. An alternative less hazardous route is to form the related dimer  $[\text{RP}(\text{S})\text{S}]_2$  ( $\text{R} = 4\text{-C}_6\text{H}_4\text{-}$

$\text{OMe}$ , **1b**). The dimer **1b**, known as Lawesson's reagent, can be readily prepared from  $\text{P}_4\text{S}_{10}$  and anisole.<sup>18</sup> Lawesson's reagent is routinely used as a thionation reagent,<sup>29</sup> but its utility as a potential dithiophosphonic complexing agent has not been previously exploited. Woollins and co-workers reported the electron-rich ferrocenyl dimer  $[\text{FcP}(\text{S})\text{S}]_2$  (**1c**) wherein Fc is the organometallic moiety.<sup>19</sup> We have prepared dithiophosphonic acid derivatives with each of the three dimers **1a–c** and alcohols and extended the chemistry further by reaction with silanols and trialkylsilanols. Once isolated, these dimers are microcrystalline solids that may be stored indefinitely in an inert atmosphere. Unsaturated (allyl), sterically demanding (adamantyl,  $\text{SiPh}_3$ , mesityl), strained (cyclopentyl), and chiral/cyclic (menthyl) are among the variety of alcohol types that have been effectively utilized in this respect. Halogen-containing and tertiary alcohols give unsatisfactory results. The former indeed forms the acid, but subsequent reaction with  $\text{NH}_3$  presumably dehydrohalogenates the acid instead of simply removing the proton from the acidic S–H moiety. The latter readily eliminates olefinic species<sup>30</sup> (Chugaev reaction) at elevated temperatures. For example,  $\text{Bu}'\text{OH}$  eliminates isobutylene.

The acids were readily transformed to the corresponding ammonium salts through reaction with dry  $\text{NH}_3$  bubbled through a concentrated benzene solution at 0 °C. Formation of the title compounds in a typical reaction was accomplished by dissolving the dithiophosphonate salt in THF, followed by addition of 1 equiv of  $\text{Au}(\text{THT})\text{Cl}$  (molar ratio 1:1) at ambient temperature. The compounds are all partly soluble to very soluble (although prone to decomposition from within a few hours to several days) in chlorinated solvents. The reaction between the dithiadiphosphetanes **1a–c** and  $[\text{Au}_2(\text{dppm})\text{Cl}_2]$  (molar ratio 1:1) in THF after 18 h yields a heterobridged dinuclear gold(I) trithiophosphonate complex of the type which **12** ( $\text{R} = \text{Fc}$ ) is typical,<sup>14a</sup> through asymmetric cleavage of the dimer<sup>31</sup> shown as follows: The



solvent was removed under vacuum, and precipitation was induced by addition of ether. Although the reaction requires considerable reaction time, it is highly efficient and the major product can be easily isolated. Although Rauchfuss and co-workers have studied reactions of Lawesson's reagent, the mechanism by which the reaction described here proceeds has not been determined.<sup>32</sup>

(28) Newallis, P. E.; Chupp, J. P.; Groenweghe L. C. D. *J. Org. Chem.* **1962**, 27, 3829 and ref 17.

(29) For reviews on Lawesson's reagent, see: (a) Cava, M. P.; Levinson, M. I. *Tetrahedron* **1985**, 41, 5061. (b) Cherkasov, R. A.; Kuttyrev, G. A.; Pudovik, A. N. *Tetrahedron* **1985**, 41, 2567. (c) Nizamov, I. S.; Batyeva, E. S.; Al'fonsov, V. A. *Russ. J. Gen. Chem.* **1993**, 63, 1840.

(30) Fackler, J. P., Jr.; Seidel, Wm. C.; Myron, M. *Chem. Commun.* **1969**, 1133.

(31) (a) Jones, R.; Williams, D. J.; Wood, P. T.; Woollins, J. D. *Polyhedron* **1987**, 539. (b) Wood, P. T.; Woollins, J. D. *Transition Met. Chem.* **1987**, 403.

**Table 5.** Dinuclear Gold(I)–Sulfur Compounds and Their Solid State Luminescence Spectral Data<sup>d</sup>

complex	298 K		77 K		Au...Au (Å)
	excitaton (nm)	emission (nm)	excitaton (nm)	emission (nm)	
[AuS <sub>2</sub> PPh(OC <sub>3</sub> H <sub>5</sub> ) <sub>2</sub> ] <sub>2</sub> , <b>7<sup>a</sup></b>	400	443	400	445, 491	3.10, 3.12
[AuS <sub>2</sub> PPh <sub>2</sub> ] <sub>2</sub> <sup>13 a</sup>	400	461	380	451, 495	2.96, 3.09
[AuS <sub>2</sub> PPh(OEt) <sub>2</sub> ] <sub>2</sub> , <b>6<sup>a</sup></b>	398	447	400	453, 496	3.10, 3.12 <sup>f</sup>
[AuS <sub>2</sub> P(4-C <sub>6</sub> H <sub>4</sub> OMe)(OEt) <sub>2</sub> ] <sup>c</sup>	392	467	395	453, 494	
[AuS <sub>2</sub> PPh(OC <sub>5</sub> H <sub>9</sub> ) <sub>2</sub> ] <sub>2</sub> , <b>2<sup>a</sup></b>	398	487	396	491, 530	2.93, 2.95
[AuS <sub>2</sub> P(O <sup>i</sup> Pr) <sub>2</sub> ] <sub>2</sub> <sup>42 a</sup>	428	450	432	468, 524	3.05, 3.10, 2.91 <sup>e</sup>
[AuS <sub>2</sub> P(4-C <sub>6</sub> H <sub>4</sub> OMe)(OSiPh <sub>3</sub> ) <sub>2</sub> ] <sub>2</sub> , <b>5<sup>b</sup></b>			319	417	3.14
[AuS <sub>2</sub> P(4-C <sub>6</sub> H <sub>4</sub> OMe)(O-menthyl) <sub>2</sub> ] <sub>2</sub> , <b>3<sup>b</sup></b>			320	447	3.04
[AuS <sub>2</sub> PEt <sub>2</sub> ] <sub>2</sub> <sup>13 b</sup>			338	423	3.18
[AuS <sub>2</sub> PMe <sub>2</sub> ] <sub>2</sub> <sup>43 b</sup>			327	421	3.19
[AuS <sub>2</sub> P(4-C <sub>6</sub> H <sub>4</sub> Me) <sub>2</sub> ] <sub>2</sub> <sup>13 c</sup>			300	418	
[Au <sub>2</sub> {S <sub>2</sub> PPh <sub>2</sub> }{(CH <sub>2</sub> ) <sub>2</sub> PMe <sub>2</sub> }] <sub>2</sub> <sup>13 b</sup>			335	451	3.10
[Au <sub>2</sub> {S <sub>2</sub> PEt <sub>2</sub> }{(CH <sub>2</sub> ) <sub>2</sub> PMe <sub>2</sub> }] <sub>2</sub> <sup>13 c</sup>			351	437	
[NBu <sub>4</sub> ] <sub>2</sub> [Au <sub>2</sub> {S <sub>2</sub> C=C(CN) <sub>2</sub> }] <sup>45 b</sup>			388	495, 527	2.80
K <sub>2</sub> [S <sub>2</sub> C=C(CN) <sub>2</sub> ]			468	553	

<sup>a</sup> Complexes with intermolecular Au...Au (~3.1 D) interactions. <sup>b</sup> Complexes with no intermolecular Au...Au interactions. <sup>c</sup> Structure not determined. For purposes of reading the text, other numbered compounds are the following: [PhP(S)S]<sub>2</sub>, **1a**; [RP(S)S]<sub>2</sub> (R = 4-C<sub>6</sub>H<sub>4</sub>OMe), **1b**; [AuS<sub>2</sub>P(Fc)(O(CH<sub>2</sub>)<sub>2</sub>O(CH<sub>2</sub>)<sub>2</sub>OCH<sub>3</sub>)<sub>2</sub>]<sub>2</sub>, **4**; [AuS<sub>2</sub>PPh(OC<sub>6</sub>H<sub>11</sub>)<sub>2</sub>]<sub>2</sub>, **8**; [AuS<sub>2</sub>PPh(O-adamantyl)<sub>2</sub>]<sub>2</sub>, **9**; [AuS<sub>2</sub>P(4-C<sub>6</sub>H<sub>4</sub>OCH<sub>3</sub>)(OCH<sub>2</sub>SiMe<sub>3</sub>)<sub>2</sub>]<sub>2</sub>, **10**; [AuS<sub>2</sub>PPh(OC<sub>6</sub>H<sub>2</sub>(CH<sub>3</sub>)<sub>3</sub>)<sub>2</sub>]<sub>2</sub>, **11**; [Au<sub>2</sub>(dppm)(S<sub>2</sub>P(S)Fc)]<sub>2</sub>, **12**. <sup>d</sup> Note that Table 4 in ref 14b incorrectly lists compound **2** and [AuS<sub>2</sub>P(O<sup>i</sup>Pr)<sub>2</sub>]<sub>2</sub> as compounds with no intermolecular interactions in the solid state. This table also presents emission data for the latter compound somewhat different from the data here taken from van Zyl's thesis. Data reported previously<sup>14b</sup> at 77 K with an excitation at 420 nm gave emission maxima at 435 and 610 nm. <sup>e</sup> The last listing is the intermolecular distance. <sup>f</sup> To be published.

**Structure.** The molecular structures of the title complexes were probed both in solution and in the solid state. Due to the asymmetry of the ligands, two different isomers (cis and trans) are possible for each new dinuclear gold(I) complex formed. Isomers are not observed for the related symmetrical S–P–S bridging ligands such as dithiophosphates, [S<sub>2</sub>P(OR)<sub>2</sub>]<sup>−</sup>, or dithiophosphinates, [S<sub>2</sub>PR<sub>2</sub>]<sup>−</sup>. The formation of the isomers, shown above, requires a more extensive structural analysis, both in solution and in the solid state. Hence these ligands are not a simple extension of the chemistry of the dithiophosphates and dithiophosphinates. In the solid state, complexes **2–5** (see Table 5 for a listing of all numbered compounds) have been analyzed with single-crystal X-ray crystallography. Complexes **2–4** are described in this study as they represent variations of both R and R' groups. The structure of **5** has been previously reported.<sup>14</sup> The complexes all have a neutral eight member metallacycle ring in an elongated chair conformation with short transannular Au...Au interactions. Complexes **2–4** crystallize with close intramolecular Au...Au interactions, with **2** by far the shortest intra- [*d*(Au...Au) = 2.926(1) Å] and intermolecular [*d*(Au...Au) = 2.954(1) Å] interaction observed to date for any dinuclear Au(I) complex with a S–P–S bridging moiety reported. The molecular structure of **2** is shown in Figure 1, and its interesting crystal packing is shown in Figure 2.

In photochemical studies performed on these complexes (vide infra), it was demonstrated that the room-temperature luminescence of **2** is quenched in chloroform, presumably by disruption of the intermolecular aurophilic interactions

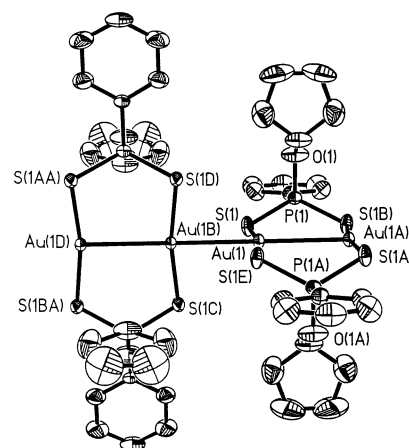


**Figure 1.** Molecular structure of complex **2** showing transannular Au...Au interactions. Thermal ellipsoids are at the 30% probability level. Hydrogen atoms are omitted for clarity.

present in the solid. Selected bond lengths and angles for **2** are shown in Table 1.

Complex **3** contains no intermolecular Au...Au interactions as shown in its crystal structure, Figure 3. The molecule crystallizes in the noncentric monoclinic space group *P2*<sub>1</sub>. The two S–Au–S linkages in the molecule are not “parallel” to each other but induce a significant “crossover” effect or twist as shown in Figure 4. The latter feature is common in open-ended dinuclear complexes (unstrained) but has not been previously observed in gold(I) metallacycles with S–P–S bridging ligands.

It is noted that **3** satisfies an important requirement for second-order NLO properties to appear with photoluminescent materials,<sup>33,34</sup> in that it crystallizes in the noncentric space group *P2*<sub>1</sub>. Noncentric space groups are relatively

(32) The expected major byproduct on the basis of stoichiometry is RP(S)Cl<sub>2</sub>. Although we obtained yields of the gold product as high as 72%, we did not look for RP(S)Cl<sub>2</sub> in the reaction mixture. Rauchfuss has discussed Lawesson's reagent as an excellent electrophile in its reaction with carbonyls and suggests it is in equilibrium with the symmetrical cleavage of RP(S)<sub>2</sub> species. Hence the mechanism for this reaction remains obscure. (a) Zank, G. A.; Rauchfuss, T. B. *Organometallics* **1984**, *3*, 1191. (b) Rauchfuss, T. B.; Zank, G. A. *Tetrahedron Lett.* **1986**, *27*, 3445.

(33) (a) Lindsay, G. A.; Singer, K. D. *Polymers for Second-Order Nonlinear Optics*; ACS Symposium Series 601; American Chemical Society: Washington, DC, 1995. (b) Zyss, J. *Molecular Nonlinear Optics*; Academic Press: New York, 1994. (c) Prasad, N. P.; Williams, D. J. *Introduction to Nonlinear Optical Effects in Molecules and Polymers*; Wiley: New York, 1991.

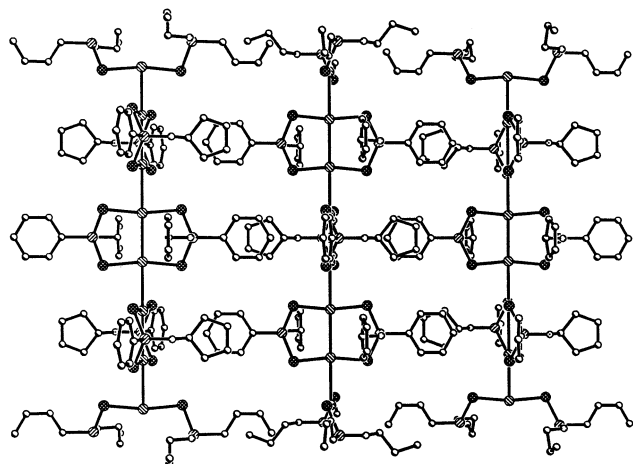


Figure 2. Crystal packing of complex 2.

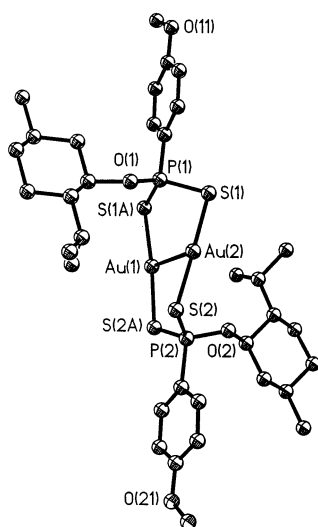


Figure 3. Molecular structure of complex 3. Thermal ellipsoids are at the 30% probability level. Hydrogen atoms are omitted for clarity.

uncommon for molecular inorganic compounds. In this case, the chiral O-menthyl containing ligand is assumed to be responsible for inducing the noncentric structure.

Complex 4 represents the first example of a ferrocenyl derivative isolated as a dithiophosphonate salt and subsequently coordinated to a transition metal center. The ether functionalities on this particular ligand may be further utilized as additional coordination sites for other metal ions, although such studies were not performed here. The molecular structure of 4 is shown in Figure 5. The cyclopentadienyl rings on both Fc groups are in the eclipsed conformation, and both Fc groups are trans to each other. It is also notable that the intramolecular Au $\cdots$ Au distances (3.08, 3.23 Å) are both different and longer than the intermolecular Au $\cdots$ Au distance (3.04 Å).

**Solid State  $^{31}\text{P}$  NMR Studies.** Since the dinuclear gold(I) complexes can form geometric cis and trans isomers, solid state  $^{31}\text{P}$  NMR studies were used to attempt to find any trace

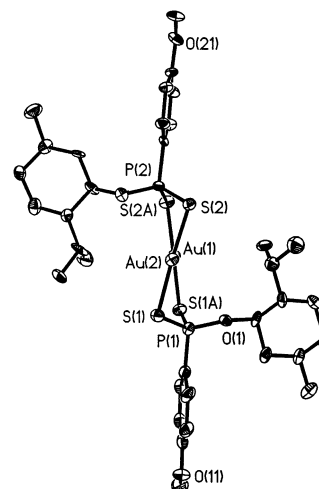


Figure 4. View of the crystal structure of complex 3 showing the crossover of the S–Au–P units.

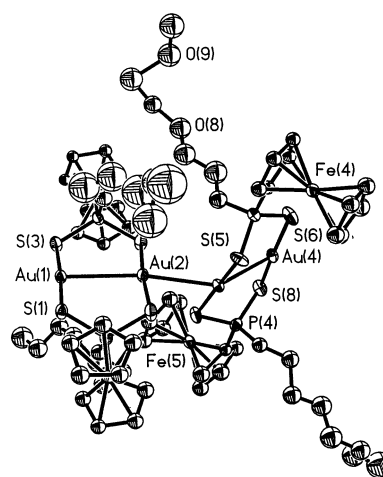


Figure 5. Molecular structure of complex 4. Thermal ellipsoids are at the 30% probability level. Hydrogen atoms are omitted for clarity.

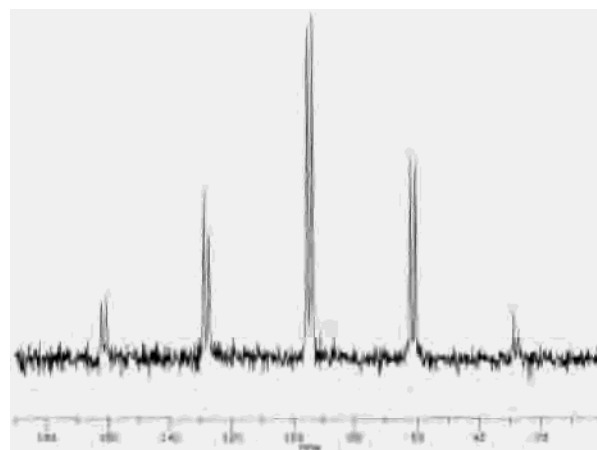


Figure 6. Solid state  $^{31}\text{P}$  NMR spectrum of complex 3.

of the cis isomer in the bulk powder. The trans isomer was exclusively present in single crystals used for X-ray studies.

The solid state  $^{31}\text{P}$  NMR powder spectrum of the noncentric 3 is shown in Figure 6. The spectrum shows singlet peaks at 95.68 and 94.06 ppm. The spinning sidebands are clearly distinguished from the relevant peaks by varying the spin rate of the rotor in two consecutive experiments with

(34) For recent reviews on NLO organometallics, see: (a) Long, N. J. *Angew. Chem., Int. Ed. Engl.* **1995**, *34*, 21. (b) Marder, S. R. In *Inorganic Materials*; Bruce, D. W., O'Hare, D., Eds.; John Wiley & Sons: New York, 1992; pp 115–164.

the same sample. Complex **3** contains discrete, well-separated dinuclear units in the solid state with negligible magnetic influence on the P atoms caused by an adjacent molecule. The structure refined in the monoclinic space group  $P2_1$  as one complete molecule in the asymmetric unit. The two phosphorus atoms in the molecule are not crystallographically nor magnetically equivalent; that is, the local environment around each P center is different and reveals a single peak for each, as is clearly the case. This is not the case in solution where both the cis and trans species each have magnetically equivalent P atoms which appear as singlets. On the basis of these observations, it was concluded that the cis isomer is *not* present in the bulk powder sample of **3** but rearrangement in solution rapidly forms it.

None of the other compounds showed the presence of the cis isomer in the solid state  $^{31}\text{P}$  NMR spectra.

**Solution NMR Studies.** Both trans and cis isomers are formed and detected in solution by NMR spectroscopy. Since the trans isomer has an inversion center and no dipole moment, and the cis isomer has no inversion center and a dipole moment, the phosphorus centers of each isomer are chemically distinct. The  $^{31}\text{P}\{^1\text{H}\}$  NMR spectrum for each of the title compounds thus reveal a singlet peak for each of the two isomers in the range 90–110 ppm, and the two peaks are usually  $\sim 1\text{--}3$  ppm apart. As expected, the  $^1\text{H}$  NMR spectrum for each complex shows the same feature as seen in the  $^{31}\text{P}\{^1\text{H}\}$  NMR spectra, namely, peaks for each isomer can be separately observed. For complexes that contain a P–Ph moiety, the phenyl group is split into two well-resolved multiplets with overlap of the peaks of the two isomers. In complexes that contain the  $\text{C}_6\text{H}_4\text{OMe}$  moiety (ligands derived from Lawesson's reagent), the OMe protons typically are found at approximately 3.8 ppm as a characteristic singlet. For **5**, very good resolution resulted in singlets at 3.81 and 3.80 ppm corresponding to the OMe protons observed for each isomer. For **4** the Cp ring attached to the phosphorus atom resulted in narrow multiplets that were centered at 4.69 and 4.50 ppm. In complex **12** the Cp protons had better resolution and similar protons were assigned as quartets (see Experimental Section). Complex **6** shows *two* quartets and *two* triplets in its  $^{31}\text{P}$  decoupled  $^1\text{H}$  NMR spectrum corresponding to the protons of the P–O–Et moiety. The spectrum shows each isomer (cis and trans) individually (as also assigned in the Experimental Section). No three-bond P–H coupling (300 MHz) was observed across the oxygen atom in the P–O–C–H type moiety (e.g. **6**) for any of the complexes.

Although all peaks for both isomers can be separately observed and accounted for in each spectrum, deciding which set of peaks corresponds to which isomer (cis or trans) was not readily possible (but see below). Variable-temperature  $^{31}\text{P}\{^1\text{H}\}$  NMR experiments were conducted but did not provide additional help. It was hoped that since the bulk powder was the trans isomer (from the structure and the solid state  $^{31}\text{P}$  NMR for **3**), a solution could be formed and cooled to prevent significant isomerization from occurring. However, two singlets were observed within seconds after dissolution at  $-80^\circ\text{C}$ , *implying that, in solution, there is a very low*

*energy barrier to isomerization.* This observation was further supported from force field calculations with the aid of CAChe molecular package, indicating a very low energy difference ( $<5$  kcal/mol) between the two isomers.<sup>35</sup> A specific isomer thus could not unambiguously be assigned to its corresponding NMR peak in this study. However, the peaks are not of the same integrated intensity and remain that way within the time of the experiment time ( $<40$  min). For all complexes, the downfield peak is always the smaller of the two.

Although solution equilibrium constants could not be accurately measured, the solution  $^{31}\text{P}\{^1\text{H}\}$  NMR intensity changes of **3** in solvents of increasing polarity are consistent with the conclusion that a rapid equilibrium between the two isomers exists. The more polar cis isomer appears to be present at  $\sim 36\%$  in the less polar solvent chloroform-*d* and at  $\sim 45\%$  in the more polar acetonitrile. On the basis of this peak intensity interpretation, the trans isomers appear at 99.7 ppm in chloroform-*d* and 102.5 ppm in acetonitrile with the cis isomers at 102 and 104 ppm in these solvents, respectively.

**Luminescence Studies.** The photophysics of  $\text{d}^{10}$  gold(I) complexes has attracted a considerable attention over the past few years.<sup>36</sup> Of special interest is the relationship between the observation of emission and the presence of weak intermolecular bonding interactions between neighboring gold centers.<sup>37</sup> The presence of such weak intermolecular metal–metal interactions has been implicated also in the design of other electronic and sensor devices.<sup>38</sup> Gold–sulfur complexes often show weak intermolecular bonding interactions (5–15 kcal/mol) between the closed-shell  $\text{d}^{10}$  gold atoms. Crystal packing effects often compete with the aurophilicity, however, and can dictate the presence or absence of aurophilic interactions in the crystalline solids. For this reason attempts have been made to determine by spectroscopy the presence of such interactions. The relationship between the observation of emission and the presence of weak intermolecular aurophilic bonding interactions between neighboring gold atoms has been addressed previously,<sup>39</sup> but a conclusive answer that applies to gold–sulfur compounds in general is yet to be obtained although some progress has been realized.<sup>14b</sup> In particular, the photolumi-

- (35) CAChe (*Computer Aided Chemistry*); CAChe Scientific, Inc., Tektronix Co.: Beaverton, OR 97077.
- (36) (a) Roundhill, D. M. *Photochemistry and Photophysics of Metal Complexes*; Plenum Press: New York, 1994. (b) King, C.; Wang, J.-C.; Khan, M. N. I.; Fackler, J. P., Jr. *Inorg. Chem.* **1989**, *28*, 2145. (c) Che, C. M.; Kwong, H. L.; Poon, C. K.; Yam, V. W. W. *J. Chem. Soc., Dalton Trans.* **1990**, 3215. (d) Li, D.; Che, C. M.; Kwong, H. L.; Yam, V. W. W. *J. Chem. Soc., Dalton Trans.* **1992**, 3235. (e) Jaw, H. R. C.; Savas, M. M.; Rogers, R. D.; Mason, W. R. *Inorg. Chem.* **1989**, *28*, 1028. (f) Hong, X.; Cheung, K. K.; Guo, C. X.; Che, C. M. *J. Chem. Soc., Dalton Trans.* **1994**, 1867. (f) Forward, J. M.; Fackler, Jr., J. P.; Assefa, Z. In *Optoelectronic Properties of Inorganic Compounds*; Roundhill, D. M., Fackler, J. P., Jr., Eds.; Plenum Press: New York, 1999; pp 195–229.
- (37) Rawashdeh-Omary, M. A.; Omary, M. A.; Patterson, H. H.; Fackler, J. P., Jr. *J. Am. Chem. Soc.* **2001**, *123*, 11237.
- (38) (a) Mansour, M. A.; Connick, W. B.; Lachicotte, R. J.; Gysling H. J.; Eisenberg, R. *J. Am. Chem. Soc.* **1998**, *120*, 1329. (b) Miller, J. S.; Epstein, A. J. *Prog. Inorg. Chem.* **1976**, *20*, 1. (c) Daws, C. A.; Exstrom, C. L.; Sowa, J. R.; Mann, K. R. *Chem. Mater.* **1997**, *9*, 363. (d) Konugi, Y.; Mann, K. R.; Miller, L. L.; Exstrom, C. L. *J. Am. Chem. Soc.* **1998**, *120*, 589.



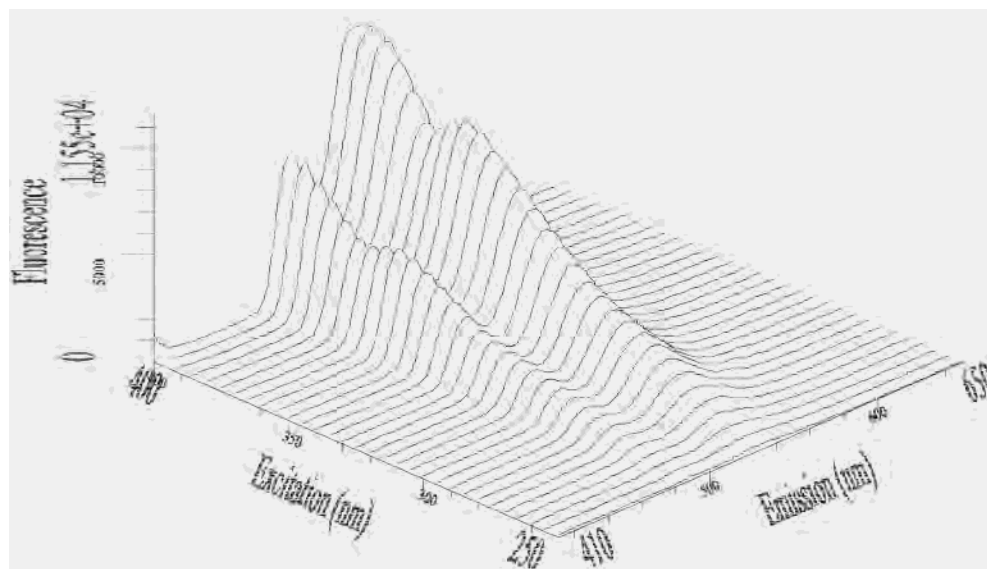


**Figure 7.** 3-D graphic of the emission spectra at 77 K of complex **2** obtained with excitations between 250 and 400 nm (increments of 5 nm).

nescence of dinuclear gold(I) dithiolate systems shows an emission that arises from a S–Au charge-transfer transition, LMCT, with contributions from the metal–metal bond formed in the excited state, LMMCT. When substituents on the sulfur ligands do not produce significant electronic perturbations, the LMMCT emission bands become strongly influenced by the intermetallic Au···Au distances.

Yam and co-workers<sup>40</sup> carefully analyzed the question of LMCT and LMMCT in a series of phosphine thiolates recently. She finds that selected ligands also contribute to the emission spectra observed, as we believe is the situation with [Au(i-MNT)<sub>2</sub>]<sub>2</sub>, where there is no aurophilic intermolecular interaction, Table 5. However, the extended chain dithiophosphonates in our study show no ligand-based low-energy emission. Hence it is reasonable to believe that LMMCT is the dominant feature of the low-energy transition observed in these extended chain species, with the M–M bond formed in the excited state strongly perturbed by intermolecular Au···Au interactions. The excited state has intermolecular contributions which lower its energy much as found in exciplex formation studies described recently for [Au(CN)<sub>2</sub>]<sup>−</sup>.<sup>37</sup> It is not clear that Yam completely ruled out a related interpretation of the solution spectra although the bulky properties of the ligands may prevent association, as found in the solid state.

This study aimed to find a clear correlation between the emission profiles of gold–sulfur complexes and the presence of weak intermolecular Au···Au interactions. The complexes studied represent a group of compounds which (i) have all been structurally characterized, (ii) all contain S–P–S bridging ligands, and (iii) are a distribution of structures with

and without *intermolecular* interactions in the solid state. These features allow direct comparisons to be made to develop a more coherent understanding of the luminescence properties of Au–S compounds. Additionally, the S–P–S bridging ligands used have been chosen not only to see if one can predict the presence or absence of intermolecular Au···Au interactions but also to qualitatively estimate the distances between the gold centers (using bulky substituents to control the distances) in cases where the emission bands have similar energies. This comparison is reliable only if the S–P–S moiety is retained for different R and OR groups attached to the phosphorus atom.

All complexes studied here luminesce at 77 K in the solid state. Several complexes (e.g. **2**, **6**, and **7**) luminesce at room temperature also and show a similar excitation and emission profile. Table 5 is a summary of the excitation and emission data measured for the complexes. Note that Table 5 replaces the Table 4 of ref 14b with better data. The observation that the emission for certain complexes (**2**, **6**, **7**) is different from that of others (**3**, **5**) suggests that the emission involves the sulfur atom of the dithiophosphonate ligand. It is not associated with  $\pi$  orbitals of the phenyl group. A large change in the energy of the emission would not be anticipated if the latter were true. Thus, these emissions as seen in **2** (Figure 7) can be assigned as ligand to metal charge transfer (LMCT), similar to results obtained with other dinuclear gold(I)–sulfur complexes.<sup>39b,40</sup> As seen in Figure 7, there are two prominent excitation energies that give rise to the two obvious emission bands, one at 360 nm and the other near 400 nm.

The blue shift observed in the emission bands with increasing temperature is consistent with an increase in Au···Au separation as a result of thermal expansion. This suggests that the Au···Au distance has a significant influence on the HOMO–LUMO gap, which increases with increasing Au···Au distance. Another observation involving these distances is that in **2**, which has the shortest inter- and intramolecular distance Au···Au of all the dithiophosphonates

(39) (a) Forward, J. M.; Bohmann, D.; Fackler, J. P., Jr.; Staples, R. J. *Inorg. Chem.* **1995**, *34*, 6330. (b) Narayanaswamy, R.; Young, M. A.; Parkhurst, E.; Ouellette, M.; Kerr, M. E.; Ho, D. M.; Elder, R. C.; Bruce, A. E.; Bruce, M. R. M. *Inorg. Chem.* **1993**, *32*, 2506. (c) Jones, W. B.; Yuan, J.; Narayanaswamy, R.; Young, M.; Elder, R. C.; Bruce, A. E.; Bruce, M. R. M. *Inorg. Chem.* **1995**, *34*, 1996.

(40) Yam, V. W.-W.; Chan, C.-L.; Li, C.-K.; Wong, K. M.-C. *Coord. Chem. Rev.* **2001**, *216–217*, 173–194.

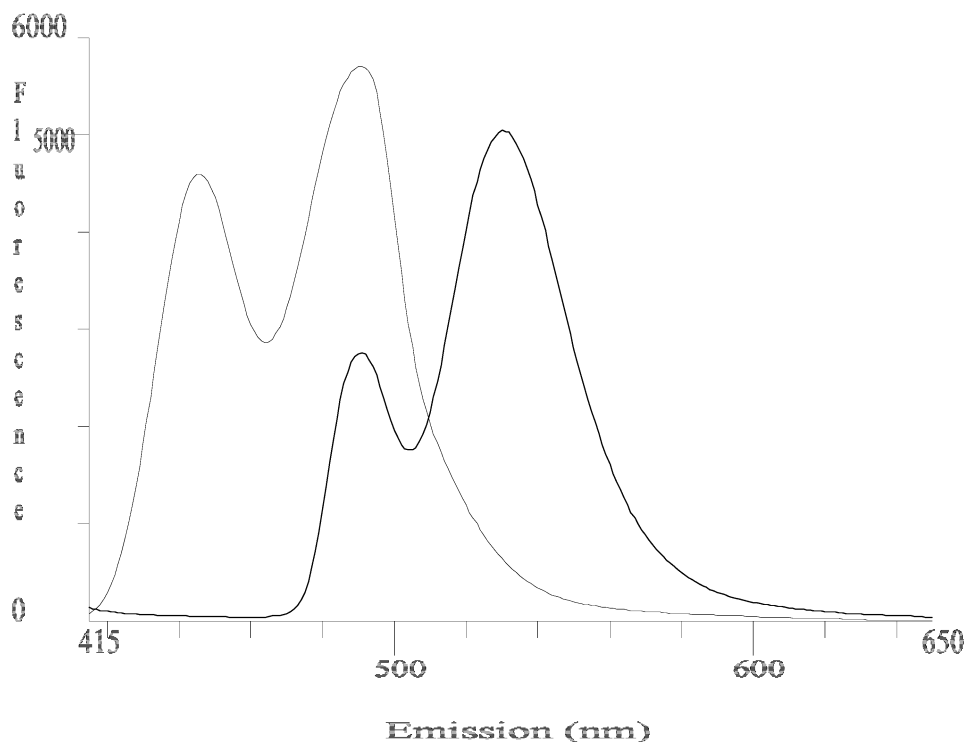


**Figure 8.** Emission spectra of complexes **2** (right) and **7** (left) indicating a significant red shift for **2** as the Au $\cdots$ Au interactions become closer in the solid state.

examined (vide supra), the emission band is significantly red shifted compared to **6** and **7**. In **6** the Au $\cdots$ Au distances are 3.096 and 3.123 Å; see Figure 8 and Table 5. The same trend is also observed between **3** and **5** in which the emission for **3**, with shorter intramolecular Au $\cdots$ Au distances, is red shifted with respect to **5**. However, this paper will not address this apparent relationship further. The donor property of the substituents on the phosphorus centers in the compounds reported here is similar; hence, they have about the same influence on the shift. Dilute CHCl<sub>3</sub> solutions ( $\sim 10^{-4}$  M) of the colored complexes (excluding R = Fc) show a disappearance of the colors (e.g. yellow **6** and **7**, green **2**), and the emission is quenched. However, concentrated solutions, in which the molecules presumably remain associated, keep their color and optical properties (Figure 8).

The absorption spectra of **7** measured at 0.1, 0.03, and 0.01 M concentrations show a progressive blue shift of the charge-transfer absorption and the disappearance of a very low intensity, broad band placed at  $\sim 400$  nm. This band corresponds to the excitation frequency producing the reported emission. Concentration-dependent UV-vis and luminescence spectra in gold(I) compounds were previously reported as evidence for molecular association in solution.<sup>40,41</sup> All of these facts seem to indicate that although the emission is related to a LMCT transition, the Au $\cdots$ Au interactions have a systematic influence on the energies of the frontier orbitals responsible for the emission. The Au $\cdots$ Au interactions produce a destabilization of the filled d<sub>z<sup>2</sup></sub> orbital (where

the z axis is along the direction of the metal–metal interaction). These Au $\cdots$ Au interactions can lead to a mixing of the empty p<sub>z</sub> orbitals on the Au centers producing a “bandlike” situation that stabilizes the LUMO. The net effect is a lowering the energy of the transition, producing the observed red shift of the emission energy. It appears consistent that as the number of Au $\cdots$ Au interactions increase, the HOMO–LUMO gap is further reduced. Thus, for example, **2**, **6**, and **7** have two different Au $\cdots$ Au interactions (inter and intra) in the solid state, while complexes such as **3** and **5** have only intramolecular interactions. The emissions of the latter are consequently blue shifted compared to **2**, **6**, and **7**. For **3** and **5** where the HOMO–LUMO gap is large (see excitation energies, Table 5), a high-energy emission does not appear.

It is proposed that the high-energy bands result from fluorescence (a small Stokes shift), while the lower energy bands result from phosphorescence (a triplet excited state). The latter band is presumably influenced strongly by the close proximity of the gold centers of different molecules because it disappears completely when there is no intermolecular Au $\cdots$ Au interaction. These results are supported by preliminary lifetime measurements performed on **2**, which contains short (2.93–2.95 Å) intermolecular Au $\cdots$ Au interactions. The blue-shifted emission peak (observed at 77 K) has a lifetime that is short (<100 ns) compared with the red-shifted peak (>500 ns). To determine if there is a general trend, the previously reported dithiophosphate complex [AuS<sub>2</sub>P(O<sup>i</sup>Pr)<sub>2</sub>]<sub>2</sub>, which shows intra- and intermolecular Au $\cdots$ Au interactions,<sup>42</sup> and [AuS<sub>2</sub>PMe<sub>2</sub>]<sub>2</sub>, which shows only intramolecular Au $\cdots$ Au interactions,<sup>43</sup> were investigated. The

(41) (a) Feng, D.-F.; Tang, S. S.; Liu, C. W.; Lin, I. J. B.; Wen, Y.-S.; Liu, L.-K. *Organometallics* **1997**, *16*, 909. (b) Fernandez, E. J.; Gimeno, M. C.; Laguna, A.; Lopez de Luzuriaga, J. M.; Monge, M.; Pykkö, P.; Sundholm, D. *J. Am. Chem. Soc.* **2000**, *122*, 7287.

luminescence properties of these complexes are consistent with results obtained in this study. For  $[\text{AuS}_2\text{P}(\text{O}^i\text{Pr})_2]_2$ , the room-temperature emission spectrum shows only one band, while at 77 K it shows two. The latter complex is nonemissive at room temperature, while at 77 K it shows one emission band at 421 nm. Recently, Eisenberg and co-workers<sup>38a</sup> reported two forms of a dinuclear gold(I) dithiocarbamate complex. The one form contains intermolecular  $\text{Au}\cdots\text{Au}$  interactions (solvated), and the other form contains no intermolecular interactions (not solvated). The luminescence properties of both forms are in accordance with the results in this study. The solvated complex shows one emission (630 nm) band and the latter shows no emission, both at room temperature. Different results are expected at 77 K for both forms; that is, the form with the one emission band at room temperature should reveal two bands, and the nonluminescent form one band.<sup>44</sup>

The ability to predict the presence of weak intermolecular  $\text{Au}\cdots\text{Au}$  interactions in other dinuclear gold–sulfur complexes from the emission spectra was tested with the complex  $[\text{NBu}_4]_2[\text{Au}_2\{\text{S}_2\text{C}=\text{C}(\text{CN})\}_2]$  for which the structure is known.<sup>45</sup> It shows no intermolecular  $\text{Au}\cdots\text{Au}$  interaction. The complex has a S–C–S bridging moiety. Surprisingly the complex shows two emission bands (495, 527 nm) at 77 K, a result that appeared to contradict the hypothesis presented in this study. Subsequent studies of the ligand showed, however, that the yellow potassium salt luminesces at 77 K with an emission at 553 nm. The 527 nm emission of the complex thus can be attributed to the ligand which has the same emission profile. This phenomenon was not seen for any of the other complexes investigated which all had colorless, nonluminescent dithiolate ligands. Hence it appears from this series of complexes studied that the

emission profile can be used to predict the presence of intermolecular  $\text{Au}\cdots\text{Au}$  interactions, at least for dinuclear gold(I)–sulfur compounds, provided that the ligand emission spectrum is known. We expect that these results can be extended to mononuclear gold(I) with sulfur ligands which may or may not be aurophilically associated.

When we reported<sup>14b</sup> the spectrum of  $[\text{AuS}_2\text{P}(\text{O}^i\text{Pr})_2]_2$ , we presented emission maxima different from those reported here.<sup>46</sup> From recent studies of Eisenberg,<sup>44</sup> it now seems likely that both data are correct and that the higher energy excitation at 77 K produces the lower energy emission.<sup>14b</sup> Similar multiple state behavior is not as apparent to date in the gold dithiophosphonate studies.

## Conclusions

This study demonstrates the facile formation of new dinuclear gold(I) dithiophosphonates from the corresponding ligand salts. The title complexes reveal two isomers in solution (cis and trans) as verified by NMR, although only the trans isomer has been found to date in the solid state. Solid state <sup>31</sup>P NMR studies performed on **3** indicate the trans isomer exclusively is present in the bulk powder, a result consistent with single-crystal structural studies. This paper shows that there is a close relationship between the structural features of the title complexes and their emission spectral profiles.

**Acknowledgment.** The authors thank the Robert A. Welch Foundation for financial support. J.M.L.-d.-L. acknowledges the University of La Rioja for financial support and two visits to Texas A&M University. Howard Patterson and C. Larochele at the University of Maine are acknowledged with thanks for some lifetime measurements, and R. T. Stubbs (TAMU) is thanked for help with X-ray crystallography in refining some structures. This paper was abstracted in part from the Ph.D. thesis of W.v.Z., Texas A&M University, Dec 1998. The authors also thank Richard Eisenberg for a preprint of work he is doing on Au(I) dithiophosphates and several helpful conversations about emission spectra.

**Supporting Information Available:** Listings of X-ray crystallographic data, all atomic coordinates, and equivalent isotropic and anisotropic parameters. This material is available free of charge via the Internet at <http://pubs.acs.org>.

IC0201856

(46) van Zyl, W. E., Ph.D. Thesis, Texas A&M University, 1998.

(42) Lawton, S. L.; Rohrbaugh, W. J.; Kokotailo, G. T. *Inorg. Chem.* **1972**, *11*, 2227.

(43) Preisenberger, M.; Bauer, A.; Schier, A.; Schmidbaur, H. *J. Chem. Soc., Dalton Trans.* **1997**, 4753.

(44) While this paper was in review, we became aware of a related study by R. Eisenberg (private communication) on alkyl dithiophosphate complexes. The structures of several dinuclear Au(I) complexes were reported along with their luminescence properties. Multiple states emission and thermochromism were observed. <sup>1</sup>MC, <sup>3</sup>MC, and <sup>3</sup>LMCT emitting states were suggested to be present from lifetime measurements. However, no direct comparison could be made between emission spectra obtained with and without intermolecular interactions since each complex in that study showed an intermolecular Au(I)⋯Au(I) interaction in the solid state.

(45) Khan, M. N. I.; Wang, S.; Fackler, J. P., Jr. *Inorg. Chem.* **1989**, *28*, 3579.